2023 IEEE International Conference on
Advanced Robotics and Its Social Impacts (ARSO)
Berlin, Germany, June 5-7, 2023

Incremental PI-like Fuzzy Logic Control of a Vacuum-Powered Artificial Muscle for Soft Exoskeletons

Esteban Centeno[1], Mijaíl Jaén Mendoza[2], Cesar F. Pinedo[3], Wangdo Kim[2], Ellen Roche[4] and Emir A. Vela[*2]

2023 IEEE International Conference on Advanced Robotics and Its Social Impacts (ARSO) | 978-1-6654-6424-6/23/$31.00 ©2023 IEEE | DOI: 10.1109/ARSO56563.2023.10187413

***Abstract*— Newborns with lower limb motor deficiencies do need rehabilitation. Soft exoskeletons based on soft artificial muscles are promising for this purpose. However, the highly non-linear dynamic behavior of their system makes very difficult to obtain an accurate model to be controlled. This paper proposes to use a free-model method called Incremental PI-Like Fuzzy logic controller (PI-Like FLC). This variation facilitates the design and interpretation of the fuzzy rules; furthermore, we were capable of using optimization algorithms and fuzzy-C-means to obtain the fuzzy sets and membership functions based on data obtained from a previously tuned PID controller. The PI-Like FLC was physically implemented on infant dummies of 0 and 6 months of age to control the knee flexion-extension motion, and a PID was used as a comparison. The results demonstrate a successful tracking control and exhibit robustness against parametric uncertainties and disturbances for both dummies' motion without the need of tuning the controller.**

I. INTRODUCTION

Introducing flexible and stretchable materials have shown promise in medical applications through a variety of soft wearable and assistive robots. Among them, a new subfield of exoskeletons have been developed using soft robotics technology. These soft exoskeletons consist of wearable garments with active mechanisms to support user motions on different parts of the body [1]-[3]. In contrast to their counterparts made of rigid materials (cable mechanism [4], DC motors [5], soft exoskeletons offer lightweight, portable and conformable systems to the user body, being an ideal wearable robotic system. Currently, most exoskeletons have been directed for adult people in physical rehabilitation and gait assistance [1], however, a few studies have centered on infants below 1 year of age since babies can also experience motor function problems [2], [6], [7]. These issues are associated to motor delay or motor paralysis, including diseases such as spina bifida or any health problem that can damage the nerve tissue in the spinal cord. One of the common treatments for non-healthy infants are passive gentle exercises on the infant's joints, in particular for new born babies affected by spina bifida [6]. Still, one of the challenges in developing an exoskeleton for babies stands for their rapid growth during the first couple of months indicating that a control scheme capable of adapting to anthropometric variations is needed.

[1]Esteban Centeno is with Dept. of Mechatronics Engineering and Mechanical Engineering, Universidad de Ingenieria y Tecnologia - UTEC, Lima, Peru luis.centeno@utec.edu.pe

[2]Mijaíl Jaén Mendoza, Wangdo Kim and Emir A. Vela* are with the Dept. of Mechanical Engineering and Research Center in Bioengineering, Universidad de Ingenieria y Tecnologia - UTEC, Universidad de Ingenieria y Tecnologia, Lima, Peru corresponding author evela@utec.edu.pe

[3]Cesar F. Pinedo is with Dept. of Mechanical Engineering, Universidad Nacional de Trujillo, Trujillo, Peru

[4]Ellen T. Roche is with the Dept. of Mechanical Engineering, MIT, Massachusetts, United States

To support user motions, the most common actuation scheme for soft exoskeletons are fluid-driven soft actuators. These have been widely used on wearable devices, especially positive pressure soft actuators that perform linear contraction [8] and bending motion [1]. This type of actuators provides high-force output for joints and ease of use, but can produce explosive failure and physical damage due to over pressurization, besides becoming bulky due to expansion. Recently, a new class of soft actuators driven by vacuum have been proposed. These vacuum actuators shrinks upon actuation instead of expanding, offering safer human-robot interactions and versatility for space-limited scenarios [9], [10]. Although vacuum actuators are a potential active scheme to perform therapy exercises in infants [11], they show a significant hysteresis and require non-linear modelling, posing limitations to closed-loop control applications.

Conventional control techniques such as model-based control strategies have been used for soft robots in continuum arms, grippers and artificial muscles [12]. For example, sliding mode control [13] and adaptive control for Festo's artificial muscle [14]. They proposed a mathematical model for their control law. Furthermore, its performance relies on the accuracy of the modelling (assumptions and simplifications) [15]. Additionally, PID control has been extensively used for demonstrations and comparisons due to its ease of implementation, working correctly within a certain range of uncertainties and nonlinearities of the system. However, there exists the possibility of presenting failures and even instability for system variations, thus being necessary to perform a new tuning of the system.

To work under uncertainty conditions, a non-model based control technique is desirable since it can respond successfully to an abrupt working condition. Neural network (NN) control were implemented successfully in a continuum robot with six actuated degrees of freedom where each joint consisted of four pneumatic chambers made of blow-molded plastic [12]; however, it had a high computational cost, its implementation was not simple, and NN depended a lot on the quality of the data that was used for training [16].

This study used a vacuum-powered artificial muscle (VPAM) that does not currently have an accurate mathematical model due to its high non-linear behavior, and which is being used to implement a soft exoskeleton for infants below 6 months old. Therefore, we present a variant of the fuzzy

Authorized licensed use limited to: Universidad Autonoma de Madrid. Downloaded on November 12,2023 at 20:13:18 UTC from IEEE Xplore. Restrictions apply.

controller called Incremental Pi-Like Fuzzy Logic Controller, which, like the conventional fuzzy controller, works without the need of a mathematical model, and its main characteristic is that its interpretation is considerably simpler because the output of the controller is the derivative of the control law and not directly the control law itself, which allows fuzzy rules to be designed much more easily for highly non-linear system dynamics. With this fuzzy controller we were capable of successfully performing the required knee flexion-extension motion of one leg for two infant dummies emulating 0 and 6 month-old infants.

II. Experimental set-up

A. Infant dummy's lower limb

The objective was to control the flexion-extension angle of an infant dummy leg produced by a VPAM simulating a knee flexion-extension rehabilitation exercise. The VPAM used on the soft exoskeleton was a bellow-type actuator that contracts by sucking its internal air. The VPAM was placed on the infant dummy's leg, anchored at the ankle and waist with the help of a pledge, all together forming a soft exoskeleton for infants (see Fig.1). This scheme was desired to lift the leg, while producing low output force in a prone position (see video). All tests were performed on two dummies made of silicone and 3D printed parts that simulated all the anthropometric conditions of the lower limbs of a zero-month-old and a six-month-old baby.

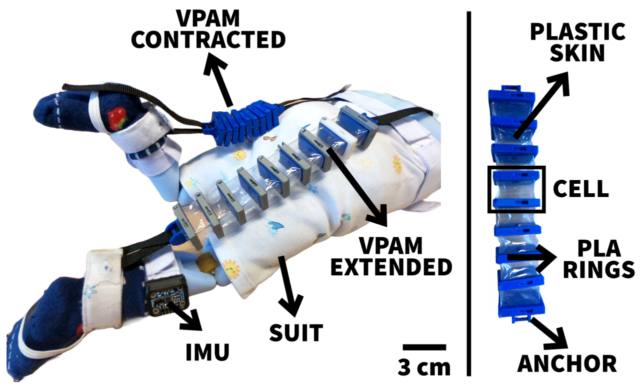

Fig. 1: Dummy used for the six-month experimental tests.

B. Vacuum-powered artificial muscle

The vacuum-powered artificial muscle used for experimental testing was lightweight, and had a rectangular cross-sectional area (30 x 15 mm). It was fabricated considering clinical specifications for rehabilitation. Each of the rings (blue parts) were slightly larger than the cross section (34.2 x 21.2 mm) with a width of 6 mm. Furthermore, they were 3D printed using a Prusa MK3s and were made of poly lactic acid (PLA). The rings were joined with a 0.1 mm thick polyethylene film, which allowed the VPAM to contract and expand. The VPAM was formed by 8 cells, each cell was formed by two rings separated by 15mm from the film (see Fig. 1). Obtaining a total muscle length of 174mm.

C. Control and feedback system

The structure of the control and feedback system can be seen in Fig. 2. An IMU (Adafruit BNO055) placed in the ankle of the dummy provided us with information about the angle of inclination of the leg and a pressure sensor placed at the inlet of the VPAM allowed to know if there was any type of pressure loss in the system, however only the IMU values were used for the control. The fuzzy controller was designed in Simulink through the serial connection between an Arduino Mega 2056 and a MATLAB program. The Fuzzy Logic Designer was used to facilitate the implementation of the controller taking advantage of Simulink tools. It should be noted that the Arduino was only used as a data acquisition board, sending the information from the sensors and receiving the required pressure (u) every 0.05 seconds.

The required pressure at each instant of time was generated with an electronic pressure regulator (SMC ITV2091-21N2BS5), powered by an air compressor (RS-2), that provided a pressure proportional to the voltage supplied to it. Finally, the voltage was supplied with a 12-bit DAC-MCP4725 that was connected to the Arduino. The cost of the entire system is approximately $700.

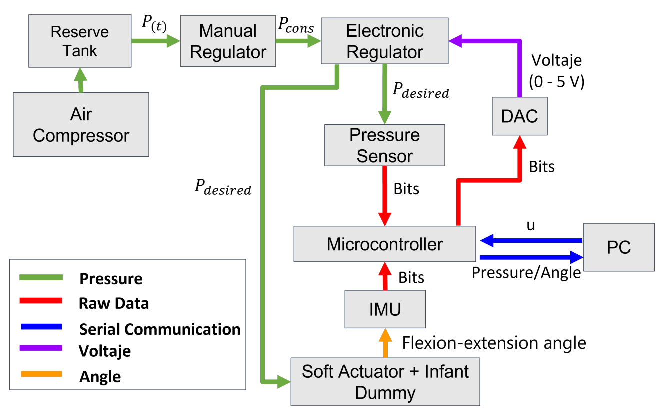

Fig. 2: Schematic of the components used for the control system, where P_i is the pressure.

III. Control strategy design

A. Incremental PI-Like Fuzzy Logic Controller structure

The structure of the controller was proposed in [17] and can be seen in Fig.3. This fuzzy controller had three linguistic variables: the error (e), the derivative of the error ($\dot{e}$) and the derivative of the pressure ($\dot{u}$) and its main advantage is that by working with $\dot{u}$ the design of the fuzzy rules is simpler, since if it is analyzed from the point of view of $\dot{u}$ one would have an interpretation such as "Increase/Reduce the pressure if ...". In addition, the integrator allowed to obtain a smooth control law at each instant of time. Fuzzy control consists of a much simpler method to implement as its design is based on the user's interpretation and this interpretation can be based on data. Furthermore, the literature demonstrated the robustness of

Authorized licensed use limited to: Universidad Autonoma de Madrid. Downloaded on November 12,2023 at 20:13:18 UTC from IEEE Xplore. Restrictions apply.

this controller and how it was very effective in working with actuators similar to the one used in this work [17].

The challenge was to perform the knee flexion-extension motion with this controller, thus imitating a therapy session that an infant affected by spina bifida would receive without the help of a professional therapist. For this, a specialist physician gave us the following clinical requirements for the therapy:

- The movement should be smooth and linear at all times, especially during extension, as there is a risk of the infant's leg hitting the surface.
- The recommended time was for flexion to last 3 seconds, extension 5 seconds and a 5 second rest time in between.
- For this study, a initial angle of 10° was considered (because this was the angle that the foot generated when it was in contact with the table). In addition, the specialist recommended that the total angle of flexion-extension should be 50° more than the initial angle (being 60° from the lying surface) and that it should not exceed 65°.

Furthermore, the controller should have the ability to operate correctly within an age range of zero to six months old without the need for modification for each month. However, since only zero and six month dummies are available, the fuzzy controller should be able to control both cases without any modification or tuning. Finally, all this was taken into account and it was used a trapezoidal signal reference modified in such a way that it complied with the given requirements.

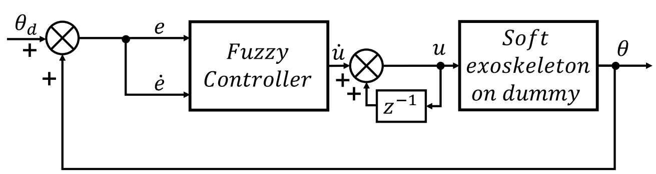

Fig. 3: Structure of the fuzzy controller of the soft exoskeleton composed of a VPAM and the garment mounted on an infant dummy. Where θ is the flexion-extension angle.

B. Data collection for design

To define the universe of discourse for each variable, experimental data from open loop and closed loop (PID) tests were used, observing graphically with histograms which were the most representative values of each variable. The following ranges were defined: [-7, 10]°, [-30, 30]°/sec and [-0.47, 0.65]kPa/sec for e, $\dot{e}$ and $\dot{u}$, respectively, because these were the ranges that contained the most representative values discarding outliers.

C. Obtaining membership functions

The fuzzy controller was of the Mandami type so it was necessary to define the fuzzy sets together with their respective membership functions. First, to define the number of fuzzy sets, the experimental data was obtained after using a manually tuned PID controller ($K_p = 0.45$, $K_i = 0.02$ and $K_d = 0.002$) that met our requirements on the six-month dummy with a trapezoidal reference and steps references ranging from 10° to 60° with jumps of 2°. This was because we needed data of the behavior of our three linguistic variables in a working range similar to the one that will work from 10° to 60°. Using the $fuzzy-C-means$ (FCM) algorithm, it was observed that five fuzzy sets managed to correctly describe the nature of each linguistic variable.

With the number of fuzzy sets defined, the membership functions (MF) of each of them had to be obtained. The same FCM algorithm was used to obtain a first idea of the distribution and shape of each MF in a quick way in order to be implemented in the $Fuzzy-Logic-Designer$ (FLD). After analyzing each linguistic variable it was observed that most of the MFs had a shape similar to that of a two-sided Gaussian, so we approximated all MFs to this type. For implementation in the FLD it was necessary to know the parameters m, σ_1 and σ_2 that describe each MF as shown in (1), where m is a known data because it is the center of each MF and the FCM gave such information.

$$\mu(x) = \begin{cases} \text{if } x \leq m & exp[-\frac{1}{2}(\frac{x-m}{\sigma_1})^2] \\ \text{if } x \geq m & exp[-\frac{1}{2}(\frac{x-m}{\sigma_2})^2] \end{cases} \quad (1)$$

Where x is the input variable, m is the center of the Gaussian, σ_1 and σ_2 are the variances of the left and right Gaussian respectively, and μ is the final membership function.

The estimation of the values of σ_1 and σ_2 can be done manually, however, it is desired to automate this process and be as accurate as possible, for that reason an optimization algorithm was used to obtain them. A simple cost function (2) was defined based on the RMS of the data obtained with FCM and the equation (1).

$$J(x) = \frac{(\mu(x) - Fcm(x))^2}{n} \quad (2)$$

Where: $J(x)$ is the value of the cost function, x is the input variable, μ is the output of the two-sided Gaussian, Fcm is the degree of membership of x with the cluster and n the number of the total data used.

D. Fuzzy rules design

The last step was to define the fuzzy rules that indicate the result of the controller depending on the input and output conditions during fuzzification and defuzzification. These rules were obtained empirically based on the experience obtained at the time of performing various tests with the VPAM, each test was analyzed to know the values of the derivative of the pressure depending on the error and the derivative of the error. The results are shown in Table I.

IV. Results

A. Step response

Fig.4 shows the performance of the PID controller (blue line) together with the fuzzy designed (red line) for a constant

Authorized licensed use limited to: Universidad Autonoma de Madrid. Downloaded on November 12,2023 at 20:13:18 UTC from IEEE Xplore. Restrictions apply.

TABLE I: Fuzzy rules defined for the controller. Where: e is the error, $\dot{e}$ the derivative of error, *PB* (Positive Big), *PS* (Positive Small) , *Ze* (Zero), *NS* (Negative Small) and *NB* (Negative Big)

e \ $\dot{e}$	**NB**	**NS**	**Ze**	**PS**	**PB**
NB	NB	NB	NB	NS	Ze
NS	NB	NS	NS	Ze	PS
Ze	NB	NS	Ze	PS	PB
PS	NS	Ze	PS	PS	PB
PB	Ze	PS	PB	PB	PB

reference of 40°. Both controllers managed to reach the value of the reference, however they had some important features:

- Both controllers needed a similar time (4.5 seconds) to stabilize, however the fuzzy has a smoother transient period, which is more suitable for a rehabilitation process.
- The control law of the fuzzy controller appeared much smoother due to the integrating effect unlike the PID which needs a high pressure from the beginning. This is due to the fact that at first a high error was generated, so the proportional component generated a high pressure to try to compensate for that error. While the fuzzy controller had the advantage of working with pressure increments from the beginning, so that it gradually increases until reaching the reference.
- The proposed fuzzy controller showed smaller tracking errors than the PID, its errors were 0.13° and 0.25° error in steady state, respectively, and without oscillations.

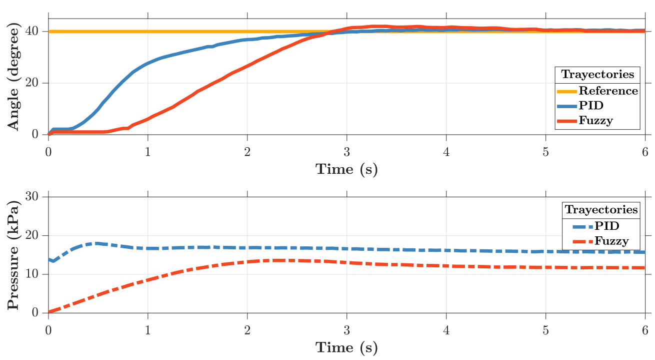

Fig. 4: Comparison of experimental results between the PID and Fuzzy controllers for a step input of 40°.

B. Anthropometric variations of the infants

Another requirement of the controller is that it must be able to work for babies in the range of zero to six months, i.e., in an environment of uncertainty. Since the leg weights of infants between zero and six months vary approximately in the range of [212, 363]g and the lengths in [93, 117]mm approximately and the controller should be able to maintain their behavior despite these changes.

In this research, different tests were performed with configurations that simulated the leg of a zero and six-month-old baby through an infant dummy legs. Fig. 5(a) shows the results obtained in both experiments, being all applied to the same trapezoidal reference without modifying any parameter of the designed controller. We can see that the results are very similar, which shows that the controller was capable of working correctly for different weights and lengths without the need of varying its design parameters or gains. Also, three main features can be highlighted:

- The six-month case required approximately 2.9 seconds for flexion and 5.4 seconds for extension. While for the zero months case it took 3.2 and 6 seconds to perform flexion and extension, respectively. And the movement was smooth at all times.
- For the six-month case it took 5 seconds to start following the reference, while for the zero-month case it only took 2.3 seconds.
- The zero-month case had a smaller stationary error at the top of the reference than the six-month case (1.63° and 0.6° respectively). However, the six-month case had no overshoot at the lower stationary stage of the reference, unlike the zero-month case which had 10% of overshoot. However, both managed to stabilize after 0.3 seconds reaching an error very close to zero (0.1°) at that stage.

Similarly, the control law generated for each case can be seen in Fig.5(b). The control law always showed a consistent smooth behavior, that was suitable for the lifetime of the electronic regulator as well as avoiding to overload the regulator. Besides, the maximum pressure values used were -16.99 and -22 kPa for the zero and six-month-old cases, respectively. In addition, both signals showed very similar and consistent behavior as expected as they worked under the same reference signal.

Just as the performance of the fuzzy controller was analyzed for anthropometric variations, the same analysis was performed for the case of the PID controller to evaluate if it was capable of controlling the system with the same conditions. Fig.6(a) shows the response of the PID controller with changes in the two month cases, the same gain was used for each case ($K_p = 0.4$, $K_i = 0.02$ and $K_d = 0.002$). The results indicated that the PID was not able to control correctly for the different months cases, showing many oscillations throughout the trajectory and indicating a potential risk to the infant. The main difference can be observed in the extension motion and in the first seconds that the knee flexion-extension began. We observed that the extension is much more prone to oscillations against small changes in the system, since a variation of 151g and 24mm (difference between weights and lengths between the legs of the dummies) were enough to generate oscillations. This was may be due to the non-linear behavior of the VPAM used and the fixed PID gains had a great impact on its dynamics or behavior.

The control law generated by the PID controller appeared to be very similar between each one of them (Fig.6(b)). The zero-month case showed an oscillatory behavior with a maximum peak pressure of -20kPa. In addition, it is seen

Authorized licensed use limited to: Universidad Autonoma de Madrid. Downloaded on November 12,2023 at 20:13:18 UTC from IEEE Xplore. Restrictions apply.

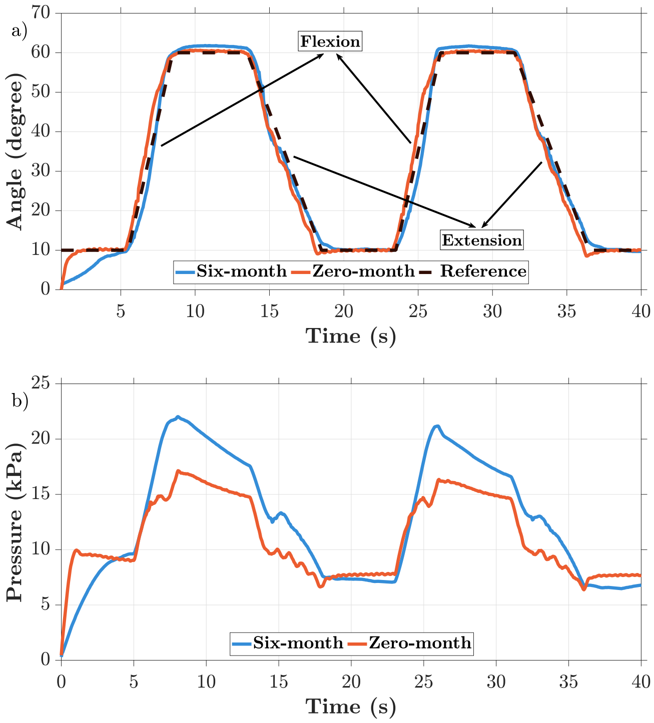

Fig. 5: Experimental results of PI-like FLC with different months, where: a) is the flexion-extension angle of the leg and b) the generated control law.

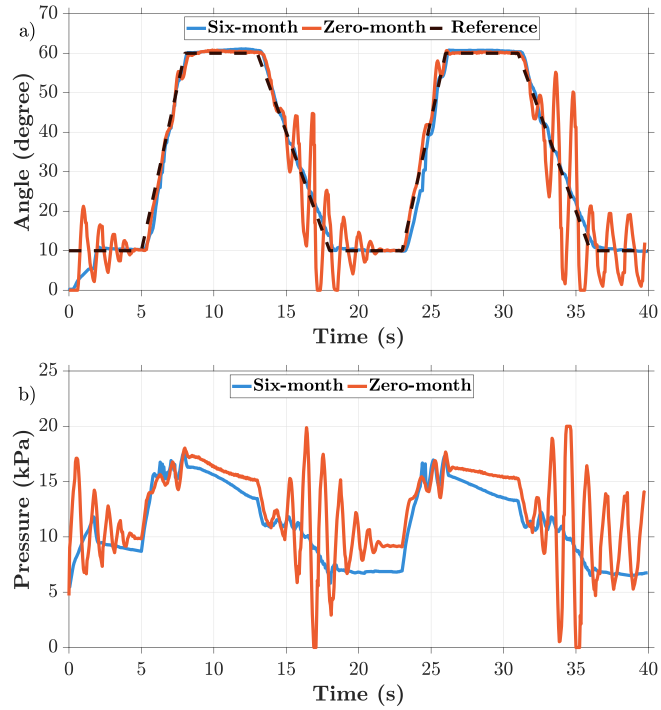

Fig. 6: Results of PID ($K_p = 0.4$, $K_i = 0.02$ y $K_d = 0.002$) with different months, where: a) is the flexion-extension angle of the leg and b) the generated control law.

that the pressure used for the six-month case was very different from the pressure shown by the fuzzy controller (see Fig.5(b)), the PID needed -17.57kPa to reach the maximum angle while the fuzzy controller needed -22kPa.

C. Response to disturbances

An additional test performed on the Fuzzy controller was the correction of a generated disturbance. In this case, the disturbance was a small bump that was exerted to the six-month dummy leg while the controller was running. Fig.7(a) shows how from one instant to the next, the leg was pushed (black rectangle) which caused the error to increase dramatically in that period time. A total of five *pushes* (simulating a small baby kick but in this case generated by manual pushes to the leg) were performed on the system: three when it was at the top (A, B, C in the graph) with different magnitudes, from a small one to a slightly stronger one; another push was performed during the flexion (D in the graph) and the last one (E in graph) was generated during the resting period at the smallest angle level.

The fuzzy controller had a fast response to these disturbances and was able to continue following the reference after they occurred. Table II summarizes the time taken by the controller to return to the reference along with its initial and final values. It is observed that for the maximum angle at A, B and C, the controller had a faster response time. For example, when a *slight* hit was executed, it took about 0.55 seconds to reach the required angular trajectory.

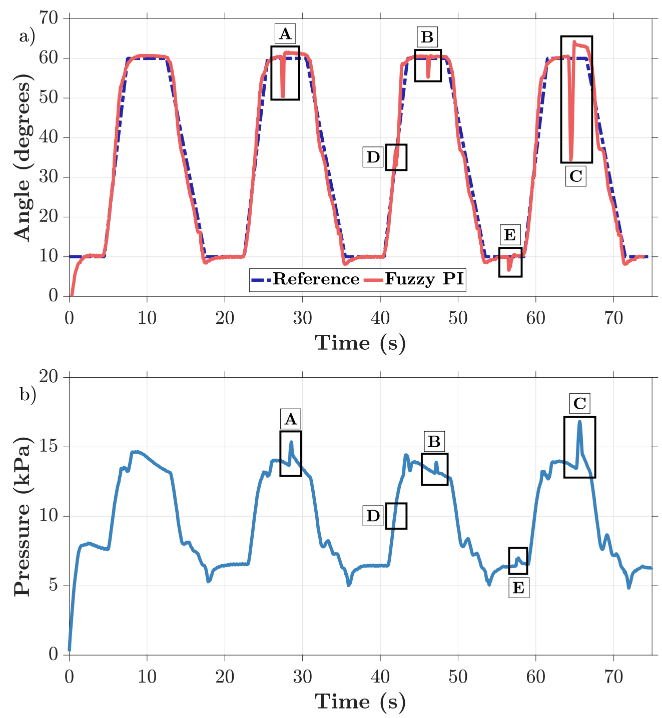

Fig. 7: Performance of the fuzzy controller against disturbances used in the six-month case. Where: a) is the flexion-extension angle of the leg, b) the generated control law and the black rectangles (A, B, C, D and E) are the instant in which the leg was pushed by hand.

Authorized licensed use limited to: Universidad Autonoma de Madrid. Downloaded on November 12,2023 at 20:13:18 UTC from IEEE Xplore. Restrictions apply.

TABLE II: Characteristics of each disturbance.

Disturbance	Reaction Time (Δt)	Angle Variation ($\Delta °$)	Pressure Variation (ΔkPa)
A	0.88	0.88	1.69
B	0.55	0.13	0.79
C	0.8	3.87	3.38
D	0.3	0.3	0.547
E	0.622	0.622	-

The steady state error in C was due to the large error induced by the bump, the fuzzy controller tried to compensate this error quickly by generating a pressure peak of -17kPa, however after overtaking the reference, the fuzzy controller was not able to decrease the angle quickly. The E case is very similar to B because its return to the reference was fast (0.622 seconds) and the difference between the angle before and after the bump was insignificant, considering that the reference was 10° at that instant.

However, this behavior was not shown in the D case, since its response was much faster than the other cases (taking 0.3 seconds to stabilize) and its difference between the angle before and after the bump was approximately 0.3°. This could be due to the fact that, unlike the other cases, the bump was excuted when the reference was still increasing, while in the other cases the reference was still constant; consequently, the required pressure was sufficient to compensate the movement caused by the external disturbance.

On the other hand, if we look at the behavior of the required pressure (or control law) in Fig.7(b), we notice an increase in pressure in the same period in which each disturbance was generated. This is expected, the controller needed much more pressure to compensate an error increment. Note that despite the disturbances, the controller behaved smoothly at all times, avoiding saturation. A summary of these values are shown in Table II, we see that the largest variation was about $3.4kPa$ in case C, the largest disturbance. The other cases showed slight variations, being D the one with the smallest variation ($0.5kPa$ approximately) and E did not generate any variation in the pressure trajectory.

V. CONCLUSION

The effectiveness and robustness of the proposed Fuzzy control method were experimentally implemented on the dummies wearing a soft exoskeleton with a new VPAM and compared against a PID controller. The experiments demonstrate that the PI-Like FLC can achieve an effective angular position control against a variation of the system parameters (mass and length of both 0 and 6-month infant dummies)) without the need of tuning for each case, unlike the PID that showed a correct performance only by tuning it for each case. It was also demonstrated that it was not necessary to obtain a mathematical model of the system to control it (complex dynamic model due to the highly non-linear behavior of VPAM), because the controller had very good performances at reaching the required angles of knee flexion-extension motion for a rehabilitation process with very small errors ($< 2°$). The non-model based PI-like FLC showed adaptability for infant models below six month of age as it can work during infant growth, opening ways to give opportunities for accessible infant rehabilitation within longer periods of time. As a next step, we will implement the controller for both legs moving alternatively.

ACKNOWLEDGMENT

This work was supported by PROCIENCIA Peru under contract N° 105-2021-FONDECYT Proyectos de Investigación Aplicada y Desarrollo Tecnológico. We thank Dr. Segundo Cruz from the National Institute of Children's Health for the discussion about clinical needs.

REFERENCES

[1] S. Sridar, P. H. Nguyen, M. Zhu, Q. P. Lam, and P. Polygerinos, "Development of a soft-inflatable exosuit for knee rehabilitation," IEEE Int. Conf. Intell. Robot. Syst., vol. 2017-Septe, pp. 3722–3727, 2017.
[2] E. Kokkoni, Z. Liu, and K. Karydis, "Development of a Soft Robotic Wearable Device to Assist Infant Reaching," J. Eng. Sci. Med. Diagnostics Ther., vol. 3, no. 2, May 2020, doi: 10.1115/1.4046397
[3] C. Di Natali et al., "Pneumatic Quasi-Passive Actuation for Soft Assistive Lower Limbs Exoskeleton," Front. Neurorobot., vol. 14, no. June, pp. 1–18, 2020.
[4] Y. L. Wang, K. Y. Wang, Y. J. Chai, Z. J. Mo, and K. C. Wang, "Research on mechanical optimization methods of cable-driven lower limb rehabilitation robot," Robotica, vol. 40, no. 1, pp. 154–169, 2022.
[5] J. Sancho-Pérez, M. Pérez, E. García, D. Sanz-Merodio, A. Plaza, and M. Cestari, "Mechanical description of ATLAS 2020, a 10-DOF paediatric exoskeleton," Adv. Coop. Robot., pp. 814–822, 2016.
[6] AsimiE. Tappit-Emas, "Spina Bifida," in Pediatric Physical Therapy, 4th Editio., Philadelphia: Lippincott Williams Wilkins, 2008, pp. 231–280.
[7] E. C. Goldfield et al., "Bio-Inspired Design of Soft Robotic Assistive Devices: The Interface of Physics, Biology, and Behavior," Ecol. Psychol., vol. 24, no. 4, pp. 300–327, Oct. 2012.
[8] Y. L. Park, J. Santos, K. G. Galloway, E. C. Goldfield, and R. J. Wood, "A soft wearable robotic device for active knee motions using flat pneumatic artificial muscles," Proc. - IEEE Int. Conf. Robot. Autom., pp. 4805–4810, 2014.
[9] S. Li, D. M. Vogt, D. Rus, and R. J. Wood, "Fluid-driven origami-inspired artificial muscles," Proc. Natl. Acad. Sci. U. S. A., vol. 114, no. 50, pp. 13132–13137, 2017.
[10] W. Felt, M. A. Robertson, and J. Paik, "Modeling vacuum bellows soft pneumatic actuators with optimal mechanical performance," 2018 IEEE Int. Conf. Soft Robot. RoboSoft 2018, pp. 534–540, 2018.
[11] M. J. Mendoza et al., "A vacuum-powered artificial muscle designed for infant rehabilitation," Micromachines, vol. 12, no. 8, pp. 1–19, 2021.
[12] P. Hyatt, D. Wingate, and M. D. Killpack, "Model-based control of soft actuators using learned non-linear discrete-time models," Frontiers Robotics AI, vol. 6, 2019.
[13] M. Luo, E. H. Skorina, W. Tao, F. Chen, S. Ozel, Y. Sun, and C. D. Onal, "Toward modular soft robotics: Proprioceptive curvature sensing and sliding-mode control of soft bidirectional bending modules," Soft Robotics, vol. 4, pp. 117 125, 6 2017.
[14] N. Sun, D. Liang, Y. Wu, Y. Chen, Y. Qin, and Y. Fang, "Adaptive control for pneumatic artificial muscle systems with parametric uncertainties and unidirectional input constraints," IEEE Transactions on Industrial Informatics, vol. 16, 2020.
[15] D. B. Reynolds, D. W. Repperger, C. A. Phillips, and G. Bandry, "Modeling the dynamic characteristics of pneumatic muscle," Annals of Biomedical Engineering, vol. 31, pp. 310–317, 2003.
[16] M. T. Gillespie, C. M. Best, E. C. Townsend, D. Wingate, and M. D. Killpack, "Learning nonlinear dynamic models of soft robots for model predictive control with neural networks," in 2018 IEEE International Conference on Soft Robotics (RoboSoft), April 2018, pp. 39–45.
[17] N. Siddique, "Intelligent control nazmul siddique a hybrid approach based on fuzzy logic, neural networks and genetic algorithms foreword by," pp. 118 119, 2013. [Online]. Available: http://www.springer.com/series/7092

Authorized licensed use limited to: Universidad Autonoma de Madrid. Downloaded on November 12,2023 at 20:13:18 UTC from IEEE Xplore. Restrictions apply.